IEEE Access
Multidisciplinary | Rapid Review | Open Access Journal

Received 23 June 2022, accepted 11 July 2022, date of publication 20 July 2022, date of current version 26 July 2022.

Digital Object Identifier 10.1109/ACCESS.2022.3192626

RESEARCH ARTICLE

Stress Grading Performance Analysis of Stator Coil Considering the Manufacturing Method and the Insulation Design

YU-MIN KIM AND MYUNGCHIN KIM
School of Electrical Engineering, Chungbuk National University, Cheongju 28644, South Korea

Corresponding author: Myungchin Kim (mckim@chungbuk.ac.kr)

This work was supported in part by the Basic Science Research Program through the National Research Foundation of Korea (NRF) funded by the Ministry of Education under Grant 2020R1A6A1A12047945, and in part by NRF Grant funded by the Korean Government through Ministry of Science and ICT (MIST) under Grant NRF-2020R1C1C1011572.

ABSTRACT In rotating machines, the approach of applying nonlinear conductive stress grading tape (SGT) has been applied to reduce the electric field stress in the coil's overhang region. To characterize and verify the electric field grading effect of SGT in electric machines, electric field analysis using the nonlinear conductivity of SGT as a boundary condition must be considered. However, previous studies have shown limitations in the characterization and application of SGT materials in insulation system design for various reasons, such as lack of conductivity measurement standards for nonlinear materials or not considering possible changes in material properties during the manufacturing procedure. In this study, the nonlinear conductivity of SGT was measured by considering the rotating machine's manufacturing procedure. A finite element method (FEM) electric field analysis was performed using the measured nonlinear conductivity. Based on the improved conductivity measurement method of SGT and FEM analysis, the effects of changing several insulation design parameters in the field grading performance were studied on a 13.8 kV stator coil. Moreover, the effect of preheating on the SGT conductivity was also examined. Based on analysis results, we realized the possibility of more precise insulation design of the stator coil. Our findings supplement the insufficient insulation design guide on the SGT part and contribute to establishing a systematic approach for insulation design. Furthermore, the proposed methods enable design optimization and detection of the cause of insulation failure.

INDEX TERMS Conductivity measurement, electric field distribution, insulation design, nonlinear conductivity, resistive field grading, rotating machine, stator coil insulation, stress grading tape.

I. INTRODUCTION

Compared to other high-voltage devices, a rotating machine has a complicated structure, and its various parts are intensively arranged such that there are many restrictions on insulation design [1]. Due to this limitation, electric field grading using a nonlinear resistance material, stress grading tape (SGT), is applied to the stator coil [1]. However, as initial physical properties of SGT could be changed during the stator manufacturing, it is necessary to consider the effect of actual manufacturing procedure to insulation design. Fig. 1(a) shows the insulation structure of the stator coil. To ensure insulation between the coils and between the coil and the core, the coils are wound with varnish impregnated insulation paper. Conductive armor tape (CAT) is wound on the outside of the insulation tape to prevent partial discharge (PD) between the grounded slot's inner surface and the coil. The CAT promotes complete grounding of the outermost coil even under the condition of point contact between the slot and the coil [2]–[4]. The CAT is applied to the entire area of the straight part of the coil and extended to the beginning of the overhang region. Since the CAT having a conductivity of 0.1 S/m or more shows characteristics similar to those of a conductor, the CAT acts as a grounding electrode, and

The associate editor coordinating the review of this manuscript and approving it for publication was Guillaume Parent.

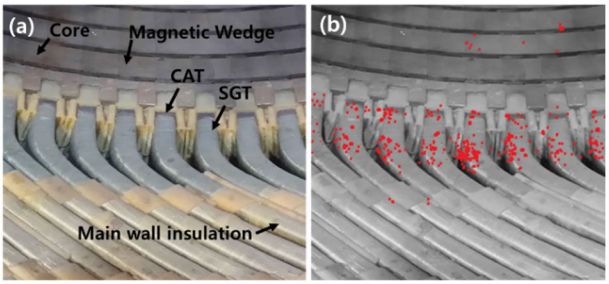

FIGURE 1. High voltage stator core. (a) insulation system and (b) PD UV (Ultraviolet) detecting test.

a high electric field can be induced at the terminal. Rotating machines using a power frequency voltage higher than 6 kV can experience PDs due to electric field concentration at the CAT's terminal [5]. To prevent such PD at the CAT's terminal of the high voltage motor coil, most high voltage motors apply the SGT [5].

Fig. 1(b) shows the creepage discharge generated on the coil detected using a UV (ultraviolet) camera. The PDs occurring at the CAT's terminal cause serious problems, such as a large amount of ozone [6], because these occur frequently in the entire overhang region of the coil. Moreover, these kinds of PDs may appear at the initial point of use or in a site acceptance test regardless of deterioration. Similar to a rotating machine, cable terminations and bushings [7] require electric field grading at the ground electrode. In the case of cables or bushings, the electric field can be reduced by using a stress cone [8] or multiple capacitor layers [9] because there is a design margin compared to the rotating machine. However, as a method for reducing the electric field at the end of the grounded CAT (or electrode) in a limited space such as a high-voltage stator coil, electric field grading using a nonlinear resistance material seems to be the most reasonable approach for electric machines [1].

Fig. 2 illustrates the concept of electric field grading by the SGT. Fig. 2(a) shows how the equipotential distribution is formed by the SGT, and Fig. 2(b) is the equivalent circuit of the impedance stress control material applied to the CAT's end. An electric field is induced by capacitance in the insulating layer, and it is also induced by resistance and capacitance in the SGT. Fig. 2(c) shows the importance of considering SGT properties during insulation design. When there is no SGT (Case A), the maximum electric field is formed in the CAT's terminal, and when the SGT is designed properly (Case C), the overall electric field is reduced. In particular, a noticeable contribution to decrease of the maximum electric field value could be achieved. However, if the conductivity of the SGT is too high or the length of the SGT is short, the electric field may be concentrated at the SGT's terminal (Case B).

Field grading of the overhang region of the stator coil is performed by the CAT and SGT. The CAT is a fiber glass tape with carbon black, and it is used to prevent slot discharge of form-wound coils [6]. The SGT plays a role in preventing the PD that occurs at the triple point of the CAT's

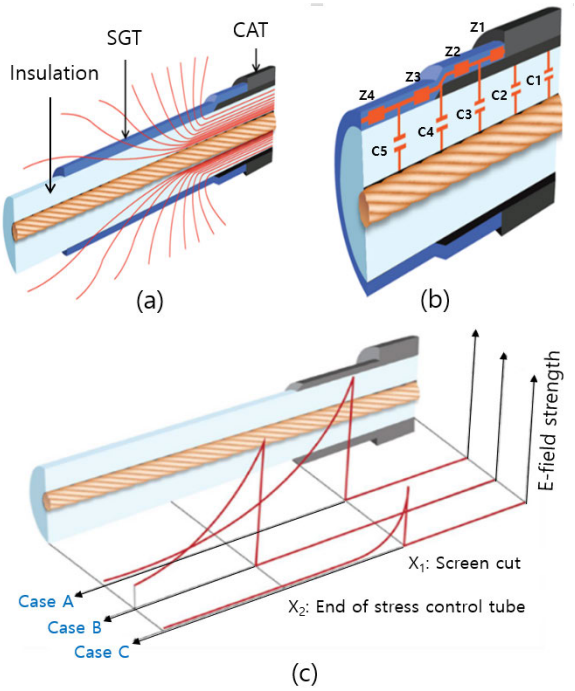

FIGURE 2. (a) Field distribution of a CAT's end with stress grading tape, (b) Equivalent circuit model of a stress grading material applied to a coil's end, (c) Effect of field grading design to electric field strength distribution between the ground and HV electrode ©2013 IEEE.(redrawn from [20]).

terminal [4]. Since the conductivity of the CAT varies depending on whether vacuum pressure impregnation (VPI) is used or not, it is necessary to measure the resistance considering the VPI [3]. The SGT is composed of resin containing silicon carbide (SiC) or zinc oxide (ZnO) varistor powder, and both types show nonlinear conductivity-field characteristics [10]. In [5], [11]–[16], the nonlinear conduction properties of the SGT were investigated for the stress grading of the overhang region; however, the VPI procedure was not addressed. In [17]–[19], the VPI procedure was considered in measuring the properties of the SGT, but the effect of heat shrinkage tape (HST) or the mica insulation layer was not considered. As with the VPI, the shrink tape and mica layers are also factors that must be considered in order to predict the actual electric field distribution. The FEM electric field analysis was performed by considering the properties of the CAT measured with or without the VPI procedure by dividing the internal and external parts of the slot in [4]. However, it seems that such study didn't consider the fact that the varnish penetrates into the slot during the VPI procedure. The SGT conductivity measurement method of previous studies may be suitable for measuring intrinsic properties, but there may be differences in the performance of the actual rotating machine. In order to calculate the practical electric field distribution using the intrinsic conductivity of the SGT, factors that were not considered in the conductivity measurement (e.g., contact resistance between the layers, varnish procedure, HST effect) should be considered in the FEM analysis.

The contributions of this current research can be discussed as follows:

First, the practical nonlinear conductivity measurement method of the SGT was employed in a rotating machine. The suggested method was thought to be suitable for calculating the practical electric field by considering the contact resistance between the layers, and the chemical reaction during the VPI and other manufacturing processes in the rotating machine. The measured properties were used as the boundary conditions in the FEM electric field analysis program COMSOL Multiphysics.

Second, the effect of insulation design on electric field distribution was studied. The design factors considered in this study are the length and thickness of the SGT and the thickness of the mica insulating layer. The quantitative review of design factors conducted in this study could contribute to development of practical guidance to manufacturers. It is also expected to be used as a basis for reviewing more diverse design factors.

Third, the SGT properties and electric field distribution according to the manufacturing process were examined. Depending on the type of SGT and the presence or absence of the preheating process of the HST, the contact characteristics of the materials are inevitably different, but there is no manufacturing guide considering this process. In this respect, the results of this study could be used as the basis for selecting an advantageous method in terms of minimizing the electric field in the existing rotating machine's process, and also for establishing a process manual.

The remainder of this paper is organized as follows: Section II presents a nonlinear conductivity measurement method that can be used for practical stator coil electric field analysis. Section III discusses the electric field distribution behavior of nonlinear resistance materials using the conductivity measurement method presented in Section II. Section IV highlights application of the proposed methods to the insulation design of the stator coil using the practical conductivity method of nonlinear conductive material and FEM analysis. Finally, Section V draws the conclusions of this study.

II. ELECTRICAL CONDUCTIVITY MEASUREMENT

Although many studies have been conducted using electric field analysis of the overhang region of the core, the actual manufacturing procedure of the rotating machine has not been considered in a comprehensive manner when measuring the material properties, which is one of the most important parameters for electric field analysis. This section introduces the theory and methodologies necessary for the rational measurement of the physical properties needed to calculate the actual distribution of a rotating electric field.

A. CONSIDERATIONS FOR NONLINEAR CONDUCTIVITY MEASUREMENTS

Electrical materials can be classified according to their electrical conductivity viz: 10^3 S/m or more as a conductor, 10^{-9}–10^3 S/m as a semiconductor, and 10^{-9} S/m or less as an insulator [21]. The most important consideration in measuring the electrical conductivity of a conductor is the contact resistance between the electrode and the material. Since the resistivity of the conductor is very small, the contact resistance at the electrode can distort the measured values of the material's properties. In order to eliminate such distortions, the electrical conductivity can be measured by the four-terminal method, the van der Pauw method, and the eddy current method, among which the four-terminal method is widely used [22]–[25]. In the case of insulators, not only the contact resistance between the electrode and the material, but also the ripple of the DC power supply, the electrical noise of the measurement environment, the stray current, and the polarization relaxation time should be considered. Among these factors, the contact resistance is a major factor in the aspect of conductors rather than insulators. In addition, the DC ripple, electrical noise, and relaxation time factors can be solved simply by using a low-ripple DC supply, shielding, grounding, and increasing the measurement time. However, preventing the stray current is difficult because it is necessary to configure an appropriate electrode system according to the magnitude of the applied voltage, the thickness of the specimen, and the measured current (creep or volume). In order to eliminate the stray current, a three-electrode system is widely used [26], [27]. In the case of semiconductors or nonlinear resistance materials, there is an ambiguity in the conductivity measurement method. In this case, not just a standardized electrode, but a suitable electrode system for each case should be devised.

Since the SGT for a rotating machine shows the properties of the semiconductor and insulator regions depending on the applied electric field, different approaches for conductivity measurement have been considered in previous studies. In [13], the conductivity measuring electrode was devised considering the shape of the stator coil. However, actual manufacturing processes such as the HST or VPI procedure were not considered. In [28], the effect of the VPI procedure on the conductivity of both the CAT and SGT were studied using electrode shapes that are suitable for conductors; the conductivity was measured by varying the temperature and applied voltage, and the measured values ranged from 1.3 to 1.6 S/m for CAT, and 5×10^{-9} to 2.5×10^{-6} S/m for SGT. Reference [4] used two types of electrodes that can measure the conductivity in the length and thickness directions of the tape. In [3], the CAT was measured in the longitudinal direction, and the SGT was measured by constructing a model coil simulating the three-electrode system of [27] on a stator coil. As described above, studies have been conducted considering major factors (e.g., SGT, CAT, temperature, varnish, etc.) in the electric field distribution of the stator coil overhang region. It is necessary to note that the field distribution of actual electric machines would be affected also by factors that are relevant to the practical design and manufacturing procedure. In this study, hence, the effect of practical factors that were not fully considered in previous studies, such as

HST, insulating layer, and preheating procedure, to the electric field distribution and conductivity characteristics of SGT were studied.

B. SAMPLE PREPARATION AND ELECTRICAL CONDUCTIVITY MEASUREMENT SYSTEM

The sample coils for measuring the nonlinear electrical conductivity of the SGT were produced in the same manner as the actual manufacturing procedure of the stator coil in a rotating machine. Since electric field grading is effective in the tangential direction of the coil's surface at the CAT's end of the stator coil, the electrode was arranged in a structure to measure the conductivity in the longitudinal direction of the SGT. Fig. 3 is a dimensional diagram of a sample for conductivity measurement. Mica tape (RikaGlase G459H, NIPPONRIKA Co.) for a rotating machine with a thickness of 0.15 mm was overlapped by a half lap on polytetrafluoroethylene(PTFE) with a diameter of 32 mm and was wound in 10 turns. The thickness of the insulating layer was selected in consideration of the strand and main wall insulation thickness of the 13.8 kV class stator coil. The distance between the electrodes was manufactured to be 30 mm and 60 mm by using an aluminum foil electrode. On the one hand, the reason that the 30 mm gap distance was selected was to apply a sufficient electric field to confirm the nonlinear switching electric field. On the other hand, considering that the length of the SGT applied to the actual stator coil in a realistic machine design would be larger than 60 mm, the sample was configured to include the 60 mm gap distance to verify whether a difference in the conductivity characteristics would occur depending on the gap length.

Two types of SGT (B-stage; 217.24, Vonroll Co. and C-stage; Rika Corovent SC-DN, NIPPONRIKA Co.) were selected for conductivity measurement. In detail, the SGT can be classified into three types based on the resin [29] viz: A-stage, B-stage, and C-stage. The A-stage is the stage before starting the reaction when the main agent and curing agent are mixed, B-stage is the stage before curing in which the main material and the curing agent are mixed to start the reaction that forms a polymer, and C-stage is the complete curing state [29]. B-stage has the advantage of excellent adhesion between the layers, but because the viscosity of the resin changes depending on the temperature, there may be differences in physical properties depending on the storage and winding procedure.

Each SGT type was overlapped by a half lap and wound in 1 turn under ideal conditions to exclude the possibility of defects in the procedure described above. On the outside of the SGT, at half overlap of the HST, 1 turn was applied. The HST was wound as a final layer in the hang over region of the stator coil machines to protect other materials during the VPI procedure. In addition, the HST shrinks at high temperatures to keep the coil insulation layers rigid. This function of the HST improves the electrical and thermal performance of the coil and prevents contamination such as dust or moisture [30].

For this reason, in this study, the HST was applied to the conductivity measurement sample to obtain results that reflect realistic configuration conditions. The manufacturing procedure of the samples is shown in Fig. 4. The model coil was manufactured in two ways: one procedure with and another one without a preheating (i.e., HTS shrinking) procedure. In order to study the effect of preheating procedure to the conductivity characteristics, a prototype for each specimen type were manufactured as shown in Table 1. As shown in Table 1, the specimen differs from each other depending on the resin type and whether preheating was applied. Preheating before impregnation was expected to prevent the SGT from washing off in the VPI procedure by shrinking the HST. It was also expected to improve electrical contact between the layers of the CAT and SGT. However, the preheating can prevent penetration of the varnish into the insulation layers. For this reason, some manufacturers perform preheating for

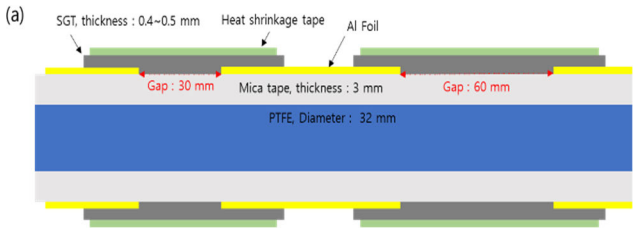

FIGURE 3. Sample coil dimensions.

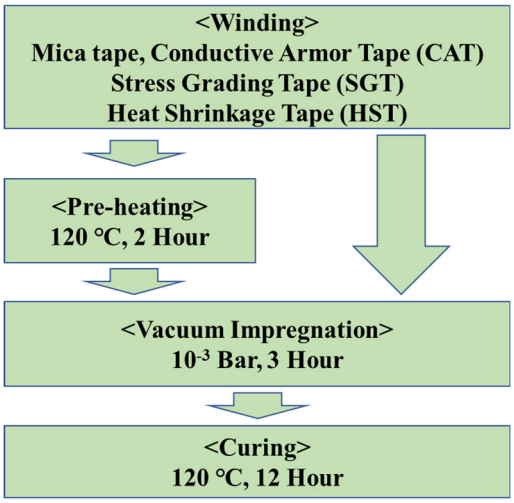

FIGURE 4. Sample preparation procedure.

TABLE 1. Description of prepared specimen.

Type	Resin Type	Preheating Application
1	B-stage	Yes
2	B-stage	No
3	C-stage	Yes
4	C-stage	No

the purpose of coil drying at a low temperature at which the HST does not shrink. Therefore, when performing preheating, various efforts are required to prevent voids inside the insulation layer, such as adjusting the temperature and VPI time of the varnish appropriately. In this study, we focused on the electrical conduction characteristics of the SGT in the presence of preheating rather than the generation of voids. As shown in Fig. 4, the entire vacuum impregnation (VI) procedure was performed except for the pressure procedure in the actual rotation VPI procedure. In the actual rotating machine procedure, the pressure procedure aims to improve the PD by reducing the void inside the varnish layer to have a size of submicron or less. Fig. 5(a) is a specimen wound by the hand layer-up method. As with the actual stator coil, wrinkles and gaps between the layers of the SGT and HST windings occurred. Fig. 5(b) shows the finished sample following the VI procedure. The bad contact and insulation distortion that occurred in the winding procedure were removed in the shrinkage procedure of the HST. From Fig. 5, it is expected that the contact resistance and conductivity of the materials will vary depending on the HST, VPI (VI), and whether the preheating procedure is performed.

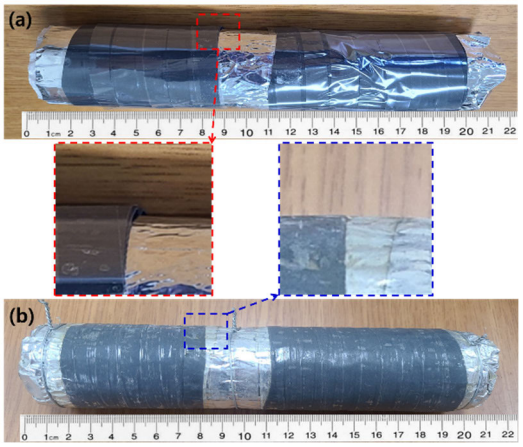

FIGURE 5. Specimen for conductivity measurement (a) after winding and (b) after Curing.

The nonlinear conductivity measurement system is shown in Fig. 6. The Kikusui company's 10 kV DC power source and Keithly company's 6485 pico-ammeter were used. The test equipment was configured to control and acquire data through the PC and GPIB(General Purpose Interface Bus) communication. For each specimen, the voltage and the current were measured and the recorded data was used for calculating the conductivity. Fig. 7 shows the nonlinear electrical conductivity of the C-stage SGT measured at inter-electrode gap distances of 30 mm and 60 mm. The conductivity was measured at a temperature of 25 °C. The gap distance required to observe the nonlinear characteristics of the SGT using a DC 10 kV source is 30 mm. Since the length of the SGT applied to the actual stator coil is more than 60 mm, it is necessary to examine whether the conductivity measured by shortening the gap distance can be applied to the electric field analysis

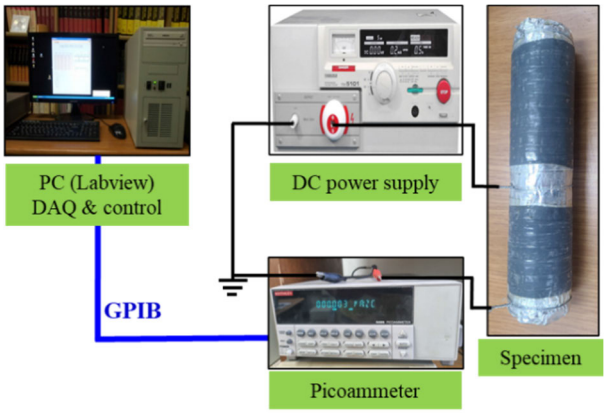

FIGURE 6. Schematic diagram for the SGT conductivity measurement.

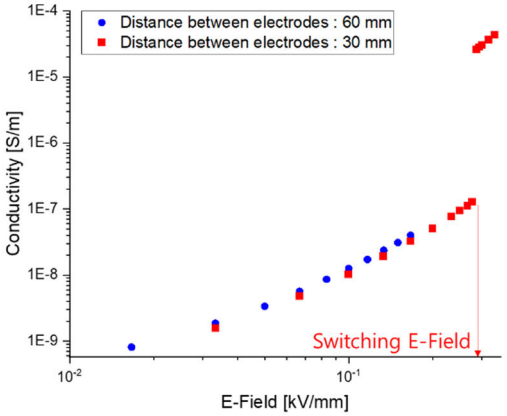

FIGURE 7. Measurement result of the nonlinear electrical conductivity of C-stage SGT according to the SGT winding length.

of the actual stator coil. It was confirmed that there was no difference in conductivity depending on the gap distance, and the data measured at 30 mm was used in subsequent studies.

C. NONLINEAR ELECTRICAL CONDUCTIVITY CHARACTERISTIC ANALYSIS

From the conductivity measurement results, a switching electric field with discontinuous conductivity at a level of about 0.25 kV/mm was observed. The nonlinear coefficient α calculated using (1) was found to have a value close to infinity according to [31]

$$\alpha = \frac{d \ln(\dot{J})}{d \ln(\dot{E})} = 1 + \frac{d \ln(\sigma)}{d \ln(\dot{E})}, \tag{1}$$

where d is differential, $\dot{J}$ is the current density, $\dot{E}$ is the electric field, and σ is the conductivity of the material. In some previous studies, the switching field was not observed [3], [6]. When SiC are used as fillers, the switching field may not be observed or the measured nonlinear coefficient may be very small [31]. This conduction characteristic is considered to be due to the nonlinear characteristic of SiC. The nonlinear properties of SiC are due to the oxide layer on the SiC surface. Pure SiC is unstable and forms an oxide layer

in the air. This oxide layer acts as an insulator between the SiC particles, and exhibits nonlinear conduction characteristics by the Schottky or tunnelling effect [30]. The ZnO varistor has the nonlinear properties of the material itself. The ZnO grain boundary formed at high temperature forms a double Schottky barrier with high nonlinearity, and has a high nonlinear coefficient [31], [32].

Looking at previous studies in which the nonlinear coefficients were measured to be small, the conductivity was estimated to be between 10^{-9} S/m and 10^{-5} S/m at 0.01 kV/mm–1 kV/mm, and a switching field was not observed [31]. The range of conductivity measured in [31] includes the boundary conductivity, $\sigma_{critical}$, which is determined as [33]

$$\sigma_{critical} = 2\pi f \varepsilon, \tag{2}$$

where f is frequency of power source, ε is the permittivity of the material and $\sigma_{critical}$ is the boundary conductivity that determines the electric field distribution by conductivity or permittivity. In the case of $\sigma_{\mathrm{SGT}} \ll \sigma_{\mathrm{critical}}$, the electric field distribution is determined according to the permittivity, and when $\sigma_{\mathrm{SGT}} \gg \sigma_{\mathrm{critical}}$, the electric field distribution is governed by conductivity. The SGT plays a role in mitigating the electric field by high conductivity in the high field region [33], [33]. When the relative permittivity $\varepsilon_{\mathrm{r}} = 10$ of a typical SGT is considered, boundary conductivity $\sigma_{\mathrm{critical}}$ that determines the governing equation of the electric field distribution becomes 2.7×10^{-8} S/m using (2).

In [3], no switching field was observed, and a conductivity in the range of 10^{-6} S/m–10^{-3} S/m was measured in the electric field range of 0.1 kV/mm–0.9 kV/mm. This value is higher than boundary conductivity $\sigma_{\mathrm{critical}}$ at the power frequency. Within the range of the measured electric field, only the electric field distribution characteristic due to conductivity can be explained. Fig. 7 shows the conductivity measurement results of C-stage SGT using the improved method. The conductivity was measured in the range of 10^{-9} S/m–10^{-4} S/m. The physical properties were measured from the insulator region to the semiconductor region, and it was considered that the analysis covering the high and low electric field region of the rotating machine SGT is possible. Moreover, a switching field was observed. There are several possibilities that explain why the results of this study are different from those of previous studies. The first is the difference according to the measurement method. Previous studies did not consider the stator coil manufacturing procedure in the conductivity measurement. In [35], a jig was considered as a method of measuring the conductivity of a conductor. However, the study did not consider the VPI procedure and the direction in which the electric field of the SGT was applied. In [4], the VPI procedure was applied in the production of samples for conductivity measurement, and a modified method from the volume resistance measurement standard [27] suitable for the SGT in rotating machines was also considered; however, the HST procedure was not considered. In this study, a jig for conductivity measurement having the same structure as the stator coil was prepared, and the VPI procedure was considered. The second may be due to differences in the SGT constituent materials. As the composition of the SGT is not known as manufacturers keep it confidential, it is necessary to look into the types of nonlinear fillers. Although the SiC is a commonly used nonlinear filler in the SGT, there are various nonlinear materials such as ZnO, $BaTiO_3/TiO_2$, and Fe_3O_4/CeO. Lastly, even if a filler with a small nonlinear coefficient and no switching field characteristics is used, there is a possibility that the switching field may be observed by the rotating machine manufacturing procedure. At the beginning of this section, the nonlinear conduction mechanism of the SiC was described. Even if the SiC was used as a nonlinear filler, the conduction mechanism at the filler interface was transferred from the Schottky effect to the tunneling effect due to the application of the HST procedure, which may show high nonlinearity.

III. ELECTRICAL FIELD ANALYSIS

A. MODELING FOR ELECTRICAL FIELD ANALYSIS

The physical properties measured in Section II were used as conductivity conditions for the FEM electric field analysis. We used the COMSOL commercial software. In Fig. 8(a), the stator coil's overhang region was modeled using the 2D axis rotation conditions as illustrated in Fig. 8(b). Fig. 8(c) is an enlarged picture of the overlapping part of the SGT and CAT in the analysis model. For FEM analysis, meshes were generated using the *physics-controlled mesh mode* and the element size options was selected as *fine* in COMSOL. Detailed studies and guidelines on optimized mesh generations are available in relevant literature [36], [37]. The size of the 13.8 kV class stator coil was considered for the dimensions of the analysis model. The strand coil was modeled as 1 mm by referring to the radius of curvature of the corner of each copper wire. Table 2 shows the permittivity values that were considered for field analysis [10], [31]. While the temperature would also have an effect to conductivity and electric field distribution [12]. [38], studies on the effect of different temperature conditions are to be explored in further work.

The voltage applied to the conductor was simulated with a 60 Hz AC. In many previous studies, pulse waveforms were applied to consider the electric field distribution by pulse width modulation (PWM) signals [3], [7], [19], [38]. Because the PWM is a power source for operating a rotating machine, it is suitable for the condition monitoring of a rotating machine and reviewing its lifespan, whereas AC power is suitable for reviewing a factory acceptance test or type test for certification [39]. As the method for measuring the physical properties of the SGT proposed in this study has not been tried, we considered AC power, not PWM, for more basic performance verification.

B. RESULTS OF ELECTRICAL FIELD ANALYSIS

Fig. 9 and Table 3 are the results of the electric field analysis performed on the 13.8 kV class stator coil with the electrical

TABLE 2. Relative permittivity values used in FEM analysis [10], [31].

Component	Coil	Mica, Varnish	ECP	SGT	Air
Relative Permittivity	1	3	100	10	1

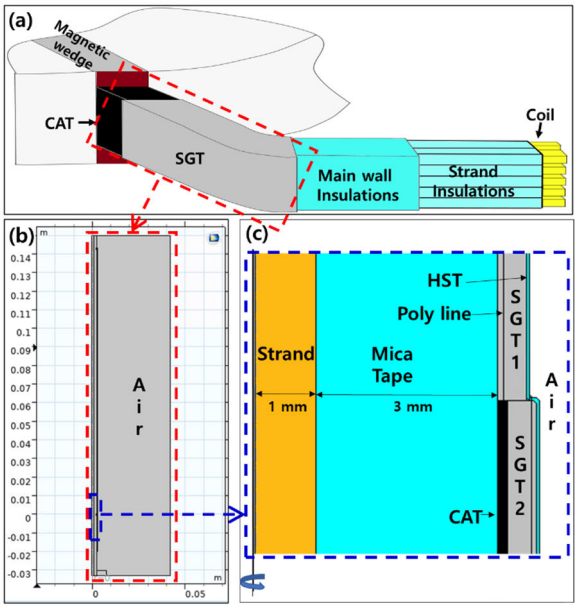

FIGURE 8. Modeling for FEM analysis. (a) schematic drawing of overhang region of stator coil [4], (b) full model for the FEM analysis, and (c) SGT, CAT overlap part.

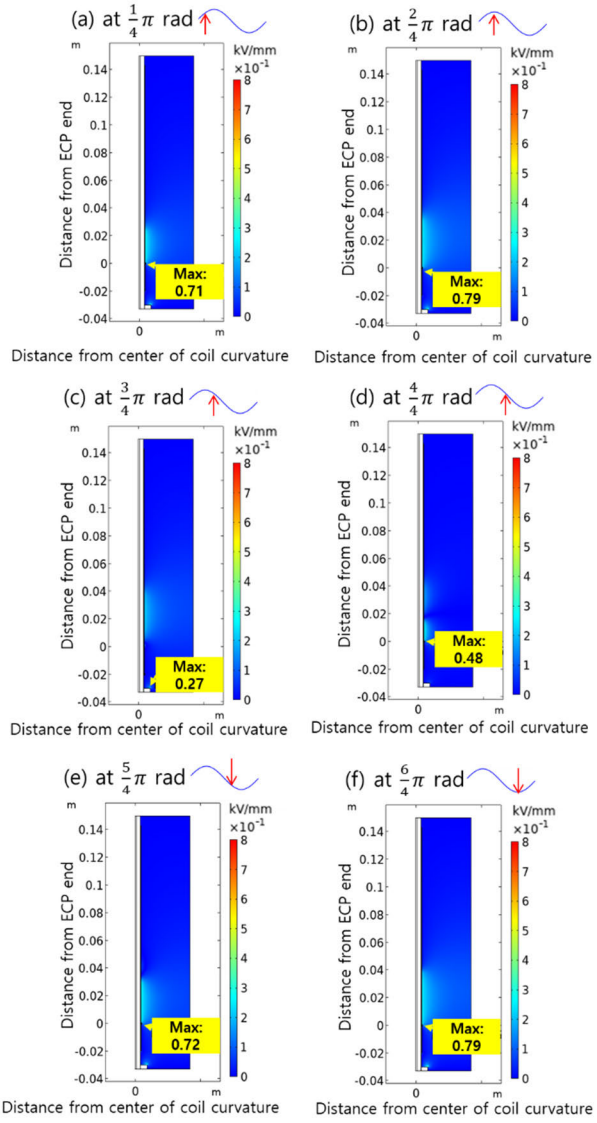

FIGURE 9. Analysis result using conductivity measured at 30 mm gap between the C-stage SGT at (a) $1/4\pi$ rad, (b) $2/4\pi$ rad, (c) $3/4\pi$ rad, (d) $4/4\pi$ rad, (e) $5/4\pi$ rad, (f) $6/4\pi$ rad.

conductivity measured at the C-stage SGT and the gap of 30 mm as the boundary condition. Since the PD at the coil terminal occurs in the longitudinal direction of the SGT, the absolute value of the component in the Z direction was considered for the electric field analysis. Although the maximum electric field differs depending on the voltage phase, it mainly occurs in the CAT terminal (Z-axis = 0 mm in Fig. 9). The reason that the maximum electric field is important is that it is a criterion for judging the occurrence of the PD. The maximum electric field of the coil's z component was calculated to be ∼0.79 kV/mm at the CAT's terminal (Z-axis = 0 mm) with $2/4\pi$ rad. The reason that the maximum electric field occurs in the CAT terminal is that a triple point is formed by the grounded CAT. In general, it is known that the dielectric breakdown strength in air is 3 kV/mm under symmetric electric field conditions [40], but the dielectric strength of air varies depending on the electric field distribution (utilization factor) and the electrode configuration [34]. In particular, Kumada *et al.* measured the corona on the surface of the stator coil and simultaneously measured it with a Pockel sensor to calculate the PD initiation field. It was found that the shorter the risetime of the applied voltage, the higher the partial discharge inception electrical field (PDIE), and that the PD occurs at 1 kHz and 0.62 kV/mm [41]. Consequently, it can be inferred that the PD will occur below 0.62 kV/mm in the power frequency domain. Inferred from the results of these previous studies, the maximum electric field of 0.79 kV/mm calculated in the FEM analysis of Fig. 9 suggests the possibility of PD. In Table 3, the length of field grading is the length of the section where the electric field is 0.25 kV/mm or more on the surface of the SGT. An electric field of 0.25 kV/mm was selected based on the switching field of the C- stage SGT in Fig. 7. The field grading section can be used as a design criterion for insulation at the applied voltage.

In order to examine the resistive electric field distribution and electric field grading of the stator coil, meanwhile, it is necessary to focus on the electric field value on the surface of the SGT except for the maximum electric field at the triple point of the CAT terminal. The reason is that the formation of

TABLE 3. Maximum electric field and conductivity grading length of SGT according to power source phase.

Sequence	Phase [Rad]	Maximum Electric Field Strength [kV/mm]	Length of field grading[mm] (>0.25 kV/mm)
(a)	$\frac{1}{4}\pi$	0.71	24
(b)	$\frac{2}{4}\pi$	0.79	34
(c)	$\frac{3}{4}\pi$	0.27	0
(d)	$\frac{4}{4}\pi$	0.48	14
(e)	$\frac{5}{4}\pi$	0.72	28
(f)	$\frac{6}{4}\pi$	0.79	34

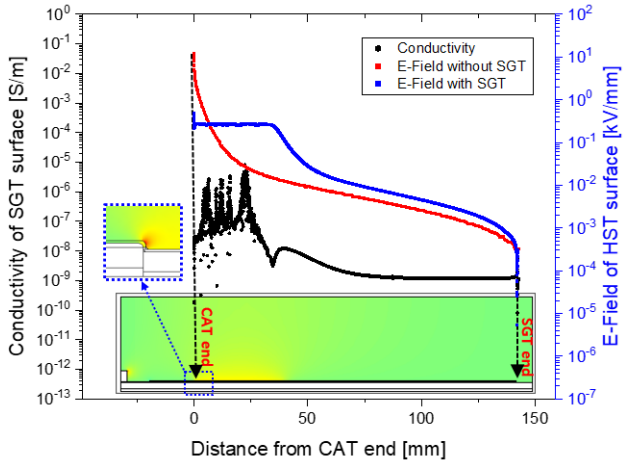

FIGURE 10. Conductivity of the SGT surface and E-Field of HST surface 2/4π [rad] of C-stage SGT.

a high electric field at the triple point depends on the electrode arrangement and shape, rather than the nonlinear properties of the SGT.

Fig. 10 shows the electric field distribution in air on the surface of the coil and the electrical conductivity of the SGT. From the difference between the electric field distribution plot, it could be seen that SGT is effective in achieving electric field grading. For the case without SGT, the maximum electric field was found be as high as 14 kV/mm at the CAT terminal. When the SGT is applied, on the other hand, the maximum electric field on the SGT surface is limited to 0.25 kV/mm. The SGT limits the maximum electric field to the switching field, which is 0.25 kV/mm for the SGT of this study, and the field is maintained until the electric field is lower below the switching field.

Also, when the electric field of the CAT terminal is increased in the absence of SGT, such as when the applied voltage is increased, the 0.25 kV/mm section will be longer. The maximum electric field on the SGT surface is limited to 0.25 kV/mm. It can be seen that the region where the electric field is 0.25 kV/mm is expanded when the voltage applied to the coil increases according to the phase. This is consistent with the measured switching field of 0.25 kV/mm in Fig. 7. In the switching electric field, the conductivity of the SGT switches from 10^{-7} S/m to 2×10^{-5} S/m, thus the resistive electric field distribution becomes effective in the high electric field region. From the position where the electrical conductivity of the SGT is 1×10^{-7} S/m or less, the electric field is dominated by the permittivity. The electric field distribution mechanism addressed in Fig. 10 was confirmed to be consistent with the electric field behavior of nonlinear conductive materials examined in [33].

IV. FIELD GRADING PERFORMANCE ANALYSIS

A. EFFECT OF INSULATION DESIGN

The insulation design factors in the stator coil of a high voltage motor include the thickness of the mica layer and SGT, and the length of the SGT. However, since the electric field analysis technology considering the conductivity of SGT, which is changed during the coil manufacturing procedure, has not been generalized, some motor manufacturers perform insulation design according to rough design guidelines; Although some manuals suggest 11 mm/kV as the design criterion for the SGT [6], this 11 mm/kV is a dimension with an excessive safety factor, which may result in waste of material and manpower. For optimal coil insulation design, the length of the SGT should be designed differently depending on the thickness of each copper wire, and the strand insulation and main insulation dimensions. By using the physical property measurement method and the electric field analysis method proposed in this study, it is possible to perform more precise study on the effect of various coil design factors on the field distribution.

Fig. 11 shows the electric field analysis results according to the length of the SGT. Fig. 11(a) is the result of analysis after applying the design standard of 11 mm/kV suggested by the SGT manufacturer, Fig. 11(b) is the case where only 1/3 of the suggested length of the SGT was applied, and Fig. 11(c) is the case where only 1/5 of the suggested length of the SGT was applied. In Fig. 11(b), the absolute value of the HST external maximum electric field is 0.75 kV/mm, and the resistive electric field grading section (the region of 0.25 kV/mm in the SGT) is 34 mm, similar to that in Fig. 11(a). In Fig. 11(c), a very high electric field was formed with an absolute value of the maximum electric field of 3.4 kV/mm. In addition, the maximum electric field was generated in the SGT's terminal, not the CAT's terminal. This is because the SGT's terminal, which shows the conductivity of the semiconductor region due to the high electric field, acted like a triple point grounded electrode. The results of Fig. 11 show that the PD at the CAT's terminal has no

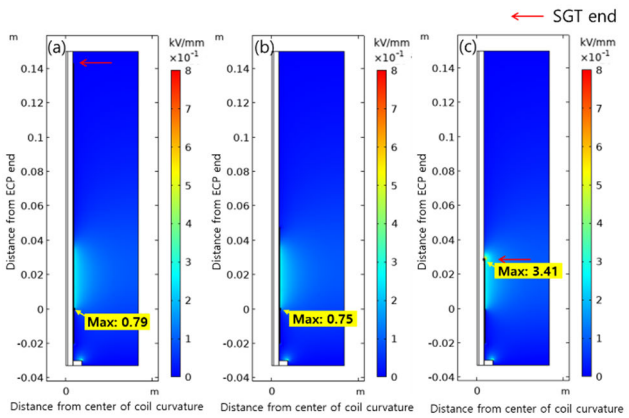

FIGURE 11. Electric field distribution along the SGT length, (a) Suggested length by the SGT manufacturer, maximum field strength is 0.79 kV/mm at the terminal of CAT, (b) 1/3 of suggested length, maximum field strength is 0.75 kV/mm at the terminal of the CAT, (c) 1/5 of suggested length, maximum field strength is 3.4 kV/mm at the terminal of the SGT.

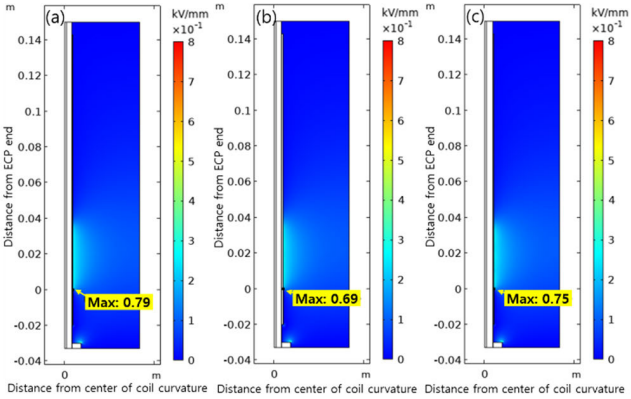

FIGURE 12. Electric field distribution, (a) Suggested thickness by the SGT manufacturer, maximum field strength is 0.79 kV/mm at the terminal of CAT (b) SGT applied twice as thick as model in (a), maximum field strength is 0.69 kV/mm at the terminal of CAT, (c) Mica tape 1.2 times thicker than that in (a) is applied, maximum field strength is 0.75 kV/mm at the terminal of CAT.

proportional relationship with the SGT's length, so it can be utilized for root cause analysis.

Fig. 12 is the result of comparing the electric field distribution according to the thickness of the SGT and mica insulating layer. Fig. 12(a) is the analysis result after applying the 13.8 kV class coil design standard proposed by the SGT supplier. Fig. 12(b) is the electric field distribution of the model designed twice as thick as the SGT in Fig. 12(a), and Fig. 12(c) is the electric field distribution of the model in which the mica insulating layer is designed to be 1.2 times thicker than that in the Fig. 12(a) model. When the SGT is thickened as in Fig. 12(b), there is no significant difference in the 0.25 kV/mm limiting electric field area, but at the CAT's terminal, the maximum electric field is reduced by ∼13% from 0.79 kV/mm to 0.69 kV/mm. Reinforcing the thickness of the SGT may be a suitable improvement if the margin for the PD test criteria is slightly insufficient. However, when

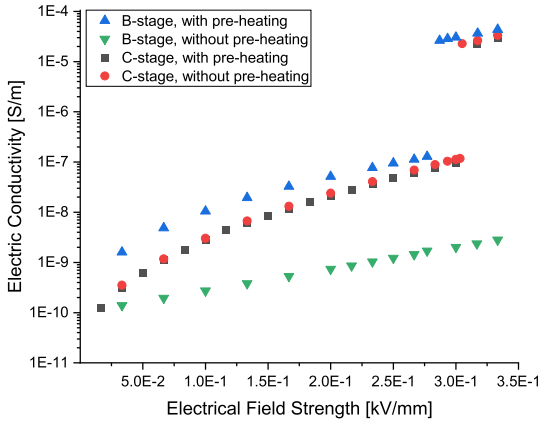

FIGURE 13. $\sigma - E$ Characteristics of the SGTs.

the mica insulating layer was 1.2 times thicker, both the improvement effect in terms of electric field distribution and maximum electric field were negligible. Although increasing the thickness of the SGT helps to minimize the electric field, it was confirmed that the thickness of the mica insulating layer had little correlation with the electric field in the longitudinal direction. The reason that the electric field relaxation effect (based on the thickness of the mica) is relatively small compared to that of the SGT is because the electric field concentration of the CAT's terminal is affected more by the shape factor of the triple point than the distance factor from the conductor.

B. EFFECT OF PREHEATING PROCEDURE

Considering that the insulation characteristics of a machine coil are affected not only by the insulation design but also by the production method, this study performed research on how the SGT properties and electric field distribution are affected by the manufacturing procedure. In particular, the effect of preheating was considered.

Fig. 13 shows the conductivity measurement result of the SGT according to the preheating procedure before impregnation. The SGTs used were the B-stage and C-stage. If the ambient temperature is high during the manufacturing procedure of the B-stage, the conductive resin may flow down. The reason for measuring the physical properties according to whether or not preheating is performed before impregnation is that the preheating procedure is different for each stator manufacturer and it may or may not be performed. The reason for not performing preheating is that if the HST shrinks due to heating, it may interfere with the penetration of the varnish in the VPI procedure, and cause void discharge inside the insulating layer. In the case of the B-stage, there was a big difference in the conductivity properties depending on whether or not preheating was performed. In the case where the preheating was not performed, the conductivity was measured to be 100 times lower than that in the case where the preheating was performed, and a switching field was not observed. This is thought to be because the nonlinear

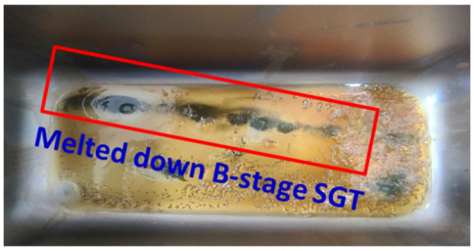

FIGURE 14. Bottom of curing oven: Melted in the curing procedure of B-stage SGT without preheating procedure.

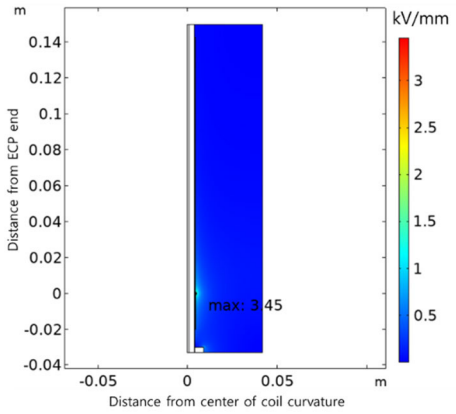

FIGURE 15. E-field Analysis results of B-stage SGT not dried before varnish impregnation.

fillers of the SGT, which had not yet been cured, were washed away in the varnish impregnation procedure. After the actual model coil was manufactured, traces of washed SGT were found at the bottom of the oven as shown in Fig. 14. In the case of an industrial curing oven, it may be difficult to detect the dissolution phenomenon of the SGT because it is larger than the model coil oven and the floor is cluttered following prolonged use.

Unlike the B-stage, the C-stage SGT showed similar electrical conductivity regardless of preheating.

Fig. 15 shows the results of electric field analysis using the conductivity properties measured in the state where the B- stage SGT was not cured in advance. The electric field grading region due to the resistive electric field distribution was not confirmed, and a high electric field of 3.4 kV/mm was calculated in the CAT's terminal. The 3.4 kV/mm calculated on the SGT's surface is ∼5 times higher than the PDIE of 0.62 kV/mm which was inferred from the results of previous studies [41], and it was considered that the possibility of partial discharge is very high.

V. CONCLUSION

To study the field grading effect of nonlinear stress grading tape (SGT) on stator coils, this study performed nonlinear conductivity measurements using model coils manufactured with the same material and manufacturing procedures as outlined for practical stator coils. With the proposed approach, both the nonlinear conductivity characteristics and the presence of the switching field were observed. In addition, based on the conductivity measurement results, an electric field analysis of the coil overhang region was performed. It was shown that the maximum electric field of the SGT near the conductive armor tape (CAT) terminal was limited by the switching field value.

The effect of several detailed factors of insulation design on the electric field distribution was also studied. It was found that the maximum electric field value was not proportional to the SGT length, and only a minimum SGT length was required for field grading. While an increase in the SGT thickness contributed to a reduction in the electric field, the thickness of the mica insulating layer had a minimal effect on the electric field in the longitudinal direction. In addition, the measurement results demonstrated changes in the conductivity characteristics of SGT depending on the manufacturing procedure, In particular, it was found that the conductivity characteristics of B-stage SGT highly depends on the application of the pre-heating procedure.

While this study focused on the impact of several factors that are relevant to insulation design and manufacturing procedure, further research on factors that are closely linked to the design and operation of realistic machines needs to be performed. Examples of such factors include structure of realistic coils and temperature changes caused by the heat. The effect of different power source waveforms (e.g., PWM and impulse), the shrinkage strength of heat shrinkage tape (HST) and winding methods also need to be studied.

REFERENCES

[1] G. C. Stone, I. Culbert, E. A. Boulter, and H. Dhirani, *Electrical Insulation for Rotating Machines: Design, Evaluation, Aging, Testing, and Repair*, Hoboken, NJ, USA: Wiley, 2004, pp. 1–370.

[2] *Insulating Systems for Large Generators*, Vonroll Co, Breitenbach, Switzerland, 2018.

[3] A. Naeini, E. A. Cherney, and S. H. Jayaram, "Effect of stress grading tape conductivity on the electric field distribution in stress grading system of an inverter-fed rotating machine," in *Proc. IEEE Electr. Insul. Conf. (EIC)*, San Antonio, TX, USA, Jun. 2018, pp. 14–17.

[4] A. Naeini, E. A. Chemey, S. H. Jayaram, and S. Ul Haq, "Effect of vacuum pressure impregnation process on electrical conductivity of conductive armor tape having various tape builds and constructions," in *Proc. IEEE Electr. Insul. Conf. (EIC)*, Baltimore, MD, USA, Jun. 2017, pp. 451–454.

[5] A. Naeini, "A study of stress grading system of medium voltage motor fed by adjustable speed drives," Ph.D. dissertation, Dept. Elect. Eng., Univ. Waterloo, Waterloo, ON, Canada, 2019.

[6] *Corona Protection CoronaShield SC 217.24.*, Vonroll Co, Breitenbach, Switzerland, 2018.

[7] F. P. Espino-Cortes, S. H. Jayaram, and E. A. Cherney, "Stress grading materials for cable terminations under fast rise time pulses," in *Proc. CEIDP Annu. Rep. Conf. Electr. Insul. Dielectric Phenomena*, Nashville, TN, USA, 2005, pp. 621–624.

[8] D. Weida, C. Richter, and M. Clemens, "Design of ZnO microvaristor material stress-cone for cable accessories," *IEEE Trans. Dielectr. Electr. Insul.*, vol. 18, no. 4, pp. 1262–1267, Aug. 2011, doi: 10.1109/TDEI.2011.5976125.

[9] M. R. Hesamzadeh, N. Hosseinzadeh, and P. Wolfs, "An advanced optimal approach for high voltage AC bushing design," *IEEE Trans. Dielectr. Electr. Insul.*, vol. 15, no. 2, pp. 461–466, Apr. 2008, doi: 10.1109/TDEI.2008.4483465.

[10] F. P. Espino-Cortes, E. A. Cherney, and S. Jayaram, "Effectiveness of stress grading coatings on form wound stator coil groundwall insulation under fast rise time pulse voltages," *IEEE Trans. Energy Convers.*, vol. 20, no. 4, pp. 844–851, Dec. 2005, doi: 10.1109/TEC.2005.853745.

[11] S. U. Haq, "A study on insulation problems in drive fed medium voltage induction motors," Ph.D. dissertation, Dept. Elect. Eng., Univ. Waterloo, Waterloo, ON, Canada, 2007.
[12] E. Sharifi-Ghazvini, "Analysis of electrical and thermal stresses in the stress relief system of inverter fed medium voltage induction motors," Ph.D. dissertation, Dept. Elect. Eng., Univ. Waterloo, Waterloo, ON, Canada, 2010.
[13] Y. Abedalla, "FEM modeling of non-linear electrical field grading for rotating machine windings," M.S. thesis, Dept. Elect. Eng., Stockholm, Sweden, 2008.
[14] A. E. Baker, "Finite element modelling of nonlinear stress grading materials for machine end windings," in *Proc. Int. Conf. Power Electron. Mach. Drives*, Bath, U.K., 2002, pp. 265–268.
[15] A. Roberts, "Stress grading for high voltage motor and generator coils," *IEEE Elect. Insul. Mag.*, vol. 11, no. 4, pp. 26–31, Jul. 1995.
[16] O. Krpal and P. Mráz, "V–A characteristic measuring of stress grading tapes in the end-winding of synchronous generators," *Proc. Eng.*, vol. 69, pp. 1523–1528, Jan. 2014, doi: 10.1016/j.proeng.2014.03.150.
[17] T. Umemoto, T. Tsurimoto, T. Kisakibaru, T. Sakurai, T. Tsuda, and K. Karasawa, "Novel evaluation methods of end-turn stress grading materials for converter-fed high voltage rotating machines," in *Proc. IEEE Conf. Electr. Insul. Dielectric Phenomena (CEIDP)*, Toronto, ON, Canada, Oct. 2016, pp. 307–310.
[18] T. Umemoto, T. Tsurimoto, S. A. Boggs, T. Kisakibaru, K. Ushiwata, and T. Yoshimitsu, "Considerations on evaluation methods for reliable stress grading systems of converter-fed high voltage rotating electrical machines," in *Proc. IEEE Conf. Electr. Insul. Dielectric Phenomena (CEIDP)*, Ann Arbor, MI, USA, Oct. 2015, pp. 47–50.
[19] T. Nakamura, A. Kumada, H. Ikeda, K. Hidaka, S. A. Boggs, Y. Tsuboi, and T. Yoshimitsu, "Transient potential measurement on stress grading under multi-level PWM," in *Proc. IEEE Electr. Insul. Conf. (EIC)*, Seattle, WA, USA, Aug. 2015, pp. 7–10.
[20] A. Eigner and S. Semino, "50 years of electrical-stress control in cable accessories," *IEEE Elect. Insul. Mag.*, vol. 29, no. 5, pp. 47–55, Sep. 2013.
[21] S. O. Kasap, "Electrical and thermal conduction in solids," in *Principles of Electronic Materials and Devices*, 3rd ed. New York, NY, USA: McGraw-Hill, 2006, pp. 154–163.
[22] M. D. Janezic, R. F. Kaiser, J. Baker-Jarvis, and G. Free, "DC conductivity measurements of metals," Nat. Inst. Standards Technol., Gaithersburg, MD, USA, NIST Tech. Note 1531, 2004.
[23] L. J. Van der Pauw, "A method of measuring specific resistivity and Hall effect of discs of arbitrary shape," *Philips Res. Rep.*, vol. 13, pp. 1–9, Feb. 1958.
[24] *Standard Test Method for Measuring Resistivity of Silicon Wafers With an In-Line Four-Point Probe*, Standard ASTM F84-98, 2003.
[25] G. Birnbaum, "Theoretical characterization and comparison of resonant-probe," in *Eddy-Current Characterization of Materials and Structures*, vol. 14, no. 6, J. B. Wheeler, Ed. Cockeysville, MD, USA: ASTM NDT International, 1981, pp. 341–342.
[26] *Insulation Resistance Measurement Handbook*, vol. 1, HIOKIKOREA Co, Seoul, South Korea, 2020, pp. 25–35.
[27] *Standard Test Methods for DC Resistance or Conductance of Insulating Materials*, Standard ASTM-D257-14(2021)e1, 2021.
[28] E. Sharifi, S. Jayaram, and E. Cherney, "Temperature and electric field dependence of stress grading on form-wound motor coils," *IEEE Trans. Dielectr. Electr. Insul.*, vol. 17, no. 1, pp. 264–270, Feb. 2010, doi: 10.1109/TDEI.2010.5412026.
[29] B. K. Appelt and P. J. Cook, "Defining B-stage and total cure for a dicy based epoxy resin by DSC," in *Analytical Calorimetry*. Boston, MA, USA: Springer, 1984, pp. 57–66.
[30] *Flexible Tapes*, Vonroll Co, Breitenbach, Switzerland, 2012.
[31] L. Donzel, F. Greuter, and T. Christen, "Nonlinear resistive electric field grading Part 2: Materials and applications," *IEEE Elect. Insul. Mag.*, vol. 27, no. 2, pp. 18–29, Mar. 2011.
[32] L. Donzel, M. Montenegro-Urtasun, and M. Hagemeister, "ZnO stress grading tape for stator windings for electrical machines located at higher altitudes," ABB, Switzerland, Tech. Rep. D1-107, 2016, pp. 1–6.
[33] T. Christen, L. Donzel, and F. Greuter, "Nonlinear resistive electric field grading Part 1: Theory and simulation," *IEEE Elect. Insul. Mag.*, vol. 26, no. 6, pp. 47–59, Nov. 2010, doi: 10.1109/MEI.2010.5599979.
[34] F. H. Kreuger, "Industrial high DC voltage: 1. fields, 2. breakdowns, 3. tests," CN, Delft, The Netherlands, Tech. Rep., 1995.
[35] R. Schmerling, F. Jenau, C. Staubach, and F. Pohlmann, "Investigations of modified nonlinear electrical materials for end corona protection in large rotating machines," in *Proc. 47th Int. Universities Power Eng. Conf. (UPEC)*, Uxbridge, U.K., Sep. 2012, pp. 6–10.
[36] E. Krusell. *Altsoft*. Belgium. Accessed: Jul. 20, 2022. [Online]. Available: https://www.comsol.com/blogs/best-practices-for-meshing-domains-with-different-size-settings/
[37] C. Zhang, S. An, W. Wang, and D. Lin, "A novel meshing method based on adaptive size function and moving mesh for electromagnetic finite element analysis," *Symmetry*, vol. 13, no. 2, pp. 2073–8994, 2021, doi: 10.3390/sym13020254.
[38] A. Naeini, E. A. Cherney, and S. H. Jayaram, "Temperature and electric field distributions along a form wound coil of an inverter-fed rotating machine with micro-varistor stress grading system," *IEEE Trans. Dielectr. Electr. Insul.*, vol. 27, no. 1, pp. 112–120, Feb. 2020, doi: 10.1109/TDEI.2019.008344.
[39] *Off-Line Partial Discharge Measurements on the Winding Insulation*, Standard IEC 60034-27-1, 2017.
[40] J. Kuffel and P. Kuffel, *High Voltage Engineering Fundamentals*, 2nd ed. Woburn, Ma, U.K.: Newnes, 2000.
[41] A. Kumada, D. Onishi, Y. Morita, T. Nakamura, K. Hidaka, S. A. Boggs, Y. Tsuboi, T. Kisakibaru, and K. Karasawa, "Surface corona inception on stress grading system in end-turn regions of rotating machines," in *Proc. 13th Int. Electr. Insul. Conf. (INSUCON)*, Birmingham, U.K., May 2017, pp. 1–6.

YU-MIN KIM was born in Janghowon, South Korea, in 1986. He received the B.S. degree in electrical engineering and the M.S. degree in high voltage engineering from Chungbuk National University, South Korea, in 2011 and 2013, respectively, where he is currently pursuing the Ph.D. degree in high voltage engineering. From 2013 to 2019, he was with Hyundai Electric and Energy System Company Ltd., Youngin, South Korea.

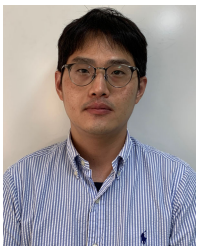

MYUNGCHIN KIM received the B.S. and M.S. degrees in electrical engineering from Hanyang University, Seoul, Republic of Korea, in 2004 and 2006, respectively, and the Ph.D. degree in electrical engineering from the University of Texas at Austin, TX, USA, in 2015. From 2006 to 2017, he was with the Agency for Defense Development, Daejeon, Republic of Korea. Since 2017, he has been with the School of Electrical Engineering, Chungbuk National University, Cheongju, Republic of Korea, where he is currently an Associate Professor. His research interests include high voltage systems, asset management, and microgrids.